Journal of Fluid Science and Technology

Vol. 5, No. 2, 2010

Response of the Fully Developed Pipe Flow to Rough Wall Disturbances (Mean Velocity Field)*

Aung Thuyein WIN**, Shinsuke MOCHIZUKI** and Takatsugu KAMEDA**

**Department of Mechanical Engineering, Yamaguchi University,
2-16-1, Tokiwadai, Ube, 755-8611, Japan.
E-mail: shinsuke@yamaguchi-u.ac.jp

Abstract

An experimental study was conducted in order to clarify the response of the fully developed pipe flow to d- and k-type wall roughness of various streamwise lengths. The measurements were set to emphasize on the response processes, which are deformation and relaxation of the mean velocity profile related to the strength and type of roughness. Under the same effective pressure drop, comparison of the mean velocity profiles and three common characteristics of boundary layer thicknesses (displacement, momentum, and energy) revealed that the initial stage of the response to the flow depends on the type of roughness. The total recovery length until the fully developed state depends only on the effective pressure drop caused by the rough wall.

Key words: Pipe Flow, Rough Wall, Response, Turbulent Structure, d-type and k-type Roughness

1. Introduction

Turbulent flow reveals its equilibrium situation which suddenly disturbed by roughness or obstacles. As passive means, wall roughness and obstacles, such as honeycomb and ring, have been examined as flow control devices. Logan and Phataraphruk[1] reported experimental data in a pipe flow disturbed by a ring. In their study, after passing over roughness element, the flow recovered in three stages (regions), namely, a jet region, an internal boundary layer region, and a similarity region. An extensive survey of the response after disturbances was presented by Smits and Wood[2], who also introduced step and impulse changes in wall surface roughness. The response of a high-Reynolds-number turbulent boundary layer to a short length of surface roughness was measured by Andreopolous and Wood[3]. The recovery condition was not observed, and the last measurement station was located at a distance of 55 times of initial boundary layer thickness from the disturbance. Moreover, one can hardly determine that the exact recovery length in a developing boundary layer flow in which the mean flow never recovers to the initial equilibrium state with an altered local skin friction coefficient. Alternatively, the turbulent pipe flow is assumed to recover after traveling a certain distance from a finite disturbance.

Obstacles located in flow fields produce momentum deficits, vortex shedding, or turbulent eddies, which complicate analysis when investigating the influences of disturbances. Various roughness types are encountered in practical flow fields. Classification is commonly based on the roughness function, which depends on the density, height, and nature of the roughness. A number of studies have investigated the distinction between d-type roughness and k-type roughness. Few studies have examined the response

*Received 15 Mar., 2010 (No. 10-0114)
[DOI: 10.1299/jfst.5.340]

to disturbances of internal flows. Leonardi et al.[4] investigated the properties of d- and k-type roughness in channel flow. They suggested that the important difference between d- and k-type roughness is the relative magnitude of frictional and pressure drag. Flow visualization on d- and k-type roughness had been made by Perry et al.[5] and summarized characteristics of d-type and k-type roughness. They found that flow over k-type roughness produce eddies with scale of roughness height, k shed into the flow and then diffused away. For d-type roughness, stable vortices form within the grooves, and there is no eddy shedding into the above boundary layer flow.

In the present study, two types of roughness, namely, d- and k-type roughness, were used to disturb a fully developed turbulent pipe flow field, and the responses of the flow were examined. The pipe flow recovers after the disturbance, provided that the recovery length is of sufficient length. The primary purpose of the present study is to distinguish between the flow structures over d- and k-type roughness and to determine the exact recovery length and its dependence on the strength of disturbance.

Nomenclatures

B	additive constant of universal log law	w_r	thickness of roughness element
b	width (groove) of roughness	x	coordinate in horizontal direction which starts from end of roughness
C_f	local friction coefficient; $C_f = \frac{\tau_w}{\frac{1}{2}\rho U_c^2} = -\frac{1}{\frac{1}{2}\rho U_c^2}\mu\left(\frac{\partial u}{\partial r}\right)_{r=R}$	x_0	coordinate in horizontal direction which starts from entrance of pipe
C_p	pressure coefficient	$x_{p,r}$	distance between peak (max.) and recovery condition of boundary layer thickness
ΔC_p	effective pressure drop		
D	Inside diameter of pipe		
k	height of roughness	x_r	recovery length
L	length of rough wall	δ_d	displacement thickness
P	static pressure	δ_e	energy thickness
P_0	reference pressure	δ_m	momentum thickness
P_w	wall static pressure	δ_i	internal boundary layer thickness
R	radius of pipe	λ	Blasius friction factor
r	coordinate in radial direction; $r = 0$ corresponds to center of pipe	κ	von Kármán constant
		ρ	density of fluid
U	mean velocity at any point of pipe	μ	dynamic viscosity
U_b	bulk mean velocity	ν	kinematic viscosity
U_c	center line (max.) velocity	τ_w	wall shear stress
u_τ	friction velocity	$^+$	denotes non-dimensionalized by wall variables
Re	Reynolds number based on pipe diameter; $U_b D/\nu$		

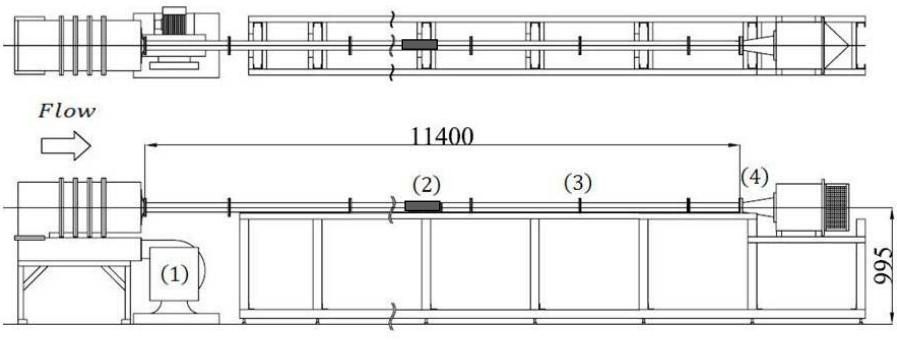

(1) *Blower* (2) *Roughness Element* (3) *Test Section* (4) *Diffuser*

Fig. 1 Experimental setup for pipe flow

2. Experimental Set-up and Technique

2.1 Pipe flow set-up

In the present study, a transparent acrylic resin pipe having an inner diameter of 70 [mm] and a total length of approximately $170D$ was used. The roughness of inner wall of the pipe varied over the length of the pipe. The experimental setup is shown in Fig. 1. The roughness section was located at $x_0 \approx 5{,}700$ [mm] ($x_0/D \fallingdotseq 80$) to ensure that the flow was fully developed. Static pressure holes of 0.5 [mm] in diameter were arranged at longitudinal and circumferential locations on the test pipe.

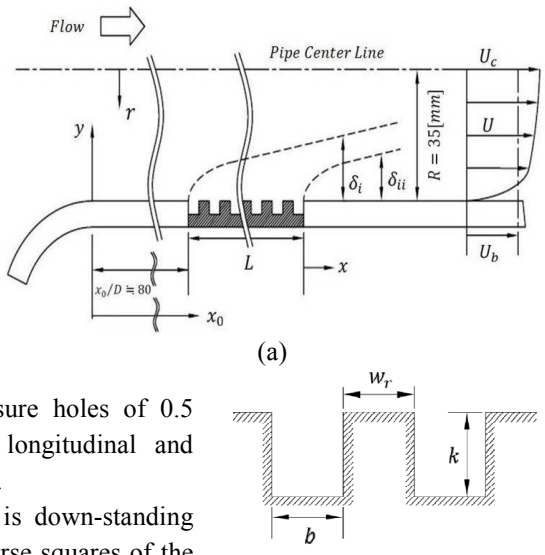

(a)

(b)

Fig. 2(a) Coordinate system and nomenclature of the flow field, (b) Sketch of roughness

The texture of the rough surface is down-standing and is constructed using circular transverse squares of the same material as the pipe. The roughness geometry is varied according to the ratio b/k , as suggested by Kameda et al.[6] and Tani et al.[7], where the groove width, b, is larger than the height, k, in order to achieve a k-type surface roughness with $b/k > 2.5$ and a d-type surface roughness with $b/k \leqq 2.5$. Detailed dimensions and the nomenclature for the surface roughnesses are listed in Table 1 and shown in Fig. 2.

Table 1 Detail dimensions of roughness

	k	w_r	b	b/k	$(b+w_r)/k$	k/R
d-type	2.5	6.25	3.75	1.5	4	0.071
k-type	2.5	3	7	2.8	4	0.071

2.2 Experimental technique and condition

The measurements of the streamwise static pressure distribution and the velocity profile were performed at $Re = U_b.D/\nu = 60 \times 10^3$. The mean velocity measurements were carried out using a squared-ended Pitot probe. The probe was aligned in the flow direction with an error of less than ±1° in order to avoid measurement errors due to the yaw effects and correction has been made according to Chue[8]. The probe was traversed by an

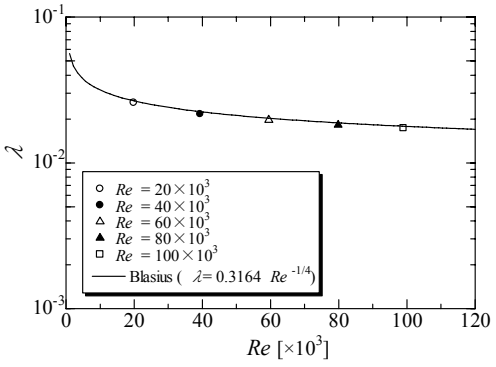

(a) Friction factor

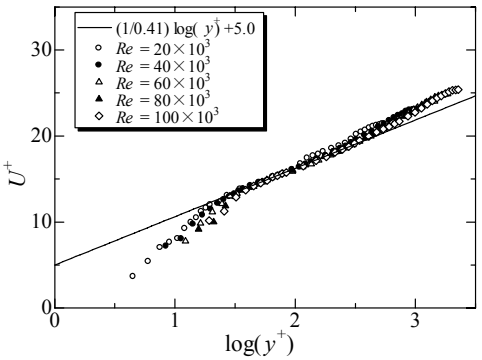

(b) Log-law profiles

Fig.3 Friction factor and mean velocity profiles

accurate positioner having a resolution of 0.01 [mm] and an accuracy of ± 0.001 [mm].

Fig. 3(a) is plotting the variation of the friction factor which was proposed by Blasius (1911) (see Benedict[9]) with Reynolds number as shown in the following,

$$\lambda = 0.3164/Re^{1/4}. \tag{2.1}$$

In this figure, experimental data of all Reynolds number well agrees with the formula proposed by Blasius within deviation of roughly 2%. The region where inner and outer are overlapping, there dimensional arguments were giving the well known log-law,

$$U^+ = \frac{1}{\kappa}\ln y^+ + B, \qquad \kappa = 0.41 \; and \; B = 5.0, \tag{2.2}$$
where $U^+ = U/u_\tau$ and $y^+ = yu_\tau/\nu$.

These classical values have been widely used for wall-bounded flows and have been confirmed to be universal to pipe flow (Nagib and Chauhan[10]). The velocity profiles normalized with the inner variables are shown in Fig. 3 for five different Reynolds numbers between 20×10^3 and 100×10^3. Figure 3(b) shows that the logarithmic velocity profiles for several Reynolds numbers are in good agreement in certain range of y^+.

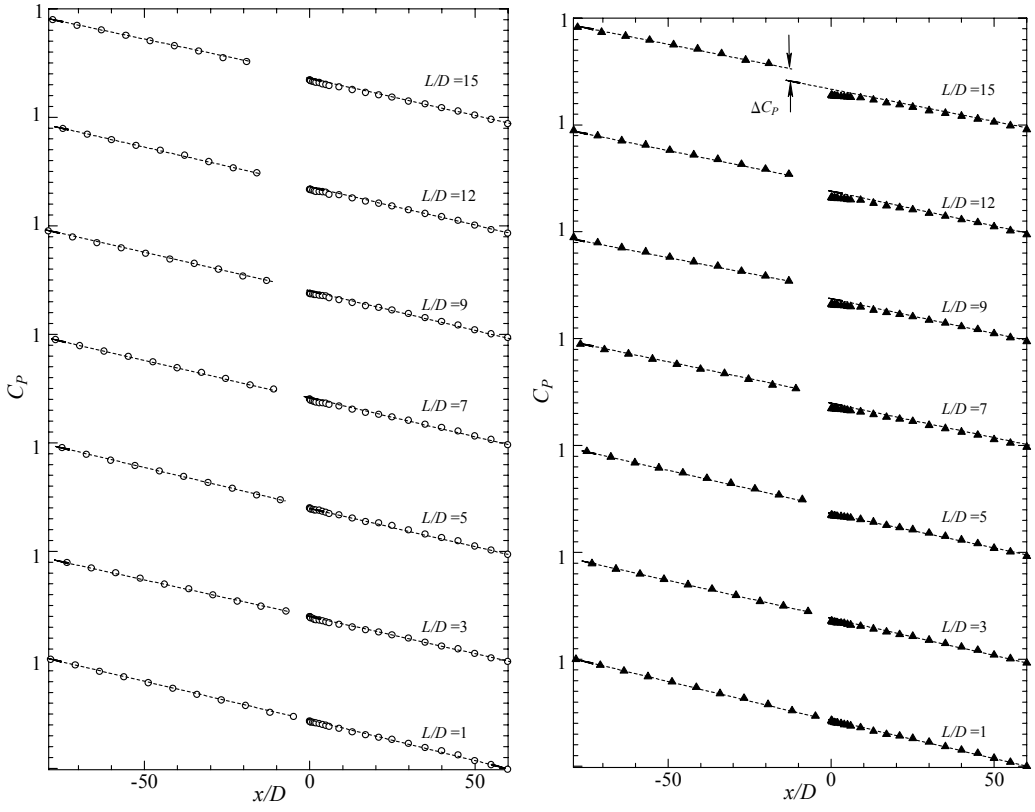

Fig. 4 Static pressure coefficient along the downstream of pipe flow; (a) d-type (b) k-type

3. Results and Discussion

3.1 Wall static pressure and mean velocity distribution

The static wall pressure coefficients were calculated using the following equation:

$$C_p = \frac{2(P_w - P_0)}{\rho U_b^2} \; . \tag{3.1}$$

where P_w is the wall static pressure; P_0 is a reference static pressure and ρ is density of fluid.

Figures 4(a) and 4(b) are the static pressure coefficients of several lengths of d- and k-type roughness, respectively. Significant pressure losses appeared because of the increases in frictional force and pressure drag force when the flow passed over the roughness section. In order to evaluate the amounts of these pressure losses, straight lines are drawn to upstream and downstream of each pressure coefficients of roughness flow, and the difference between the height of the two straight lines is determined. The results are shown with respect to the roughness length in Fig. 5.

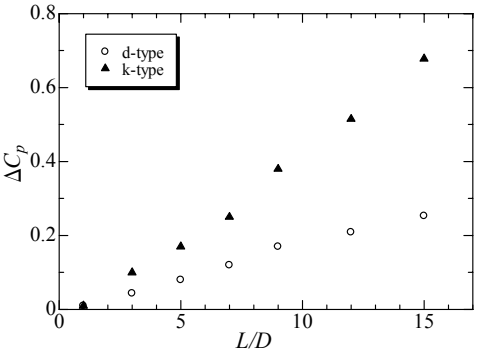

Fig. 5 Static pressure difference against two types of roughness varying in length

The effective pressure drop due to the presence of roughness, ΔC_p (referred to hereinafter as effective pressure drop) is an indication of the roughness as a disturbance. Comparison of ΔC_p for two types of roughness yields important information that differs according to the nature and strength of the roughness. In Fig. 5, in comparing ΔC_p, there are two conditions appearing nearly same values of the effective pressure drop, $L/D = 9$ (d-type) and $L/D = 5$ (k-type), $L/D = 15$ (d-type) and $L/D = 7$ (k-type), respectively.

Comparison has been made on the mean velocity profiles of undisturbed and disturbed flows which are based on the same effective pressure drop for d-type ($L/D = 15$) and k-type ($L/D = 7$) are shown in Fig. 6. The solid line represents the undisturbed fully developed flow (smooth wall). The roughness induced an additional friction force and

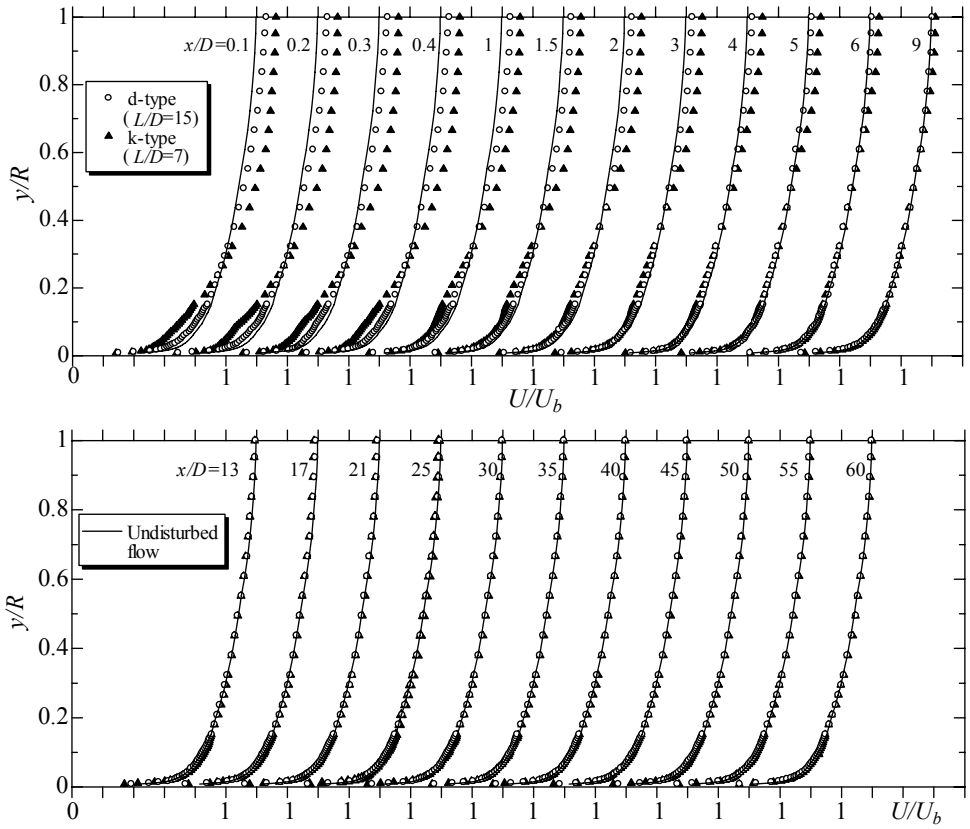

Fig. 6 Comparison of deformation and recovery process of the mean velocity profile under the same effective pressure drop

increased the velocity deficit near the wall. Downstream of the roughness, the deformation of the d-type roughness flow is smaller than that of the k-type roughness. At the pipe center, the mean flow is faster until the point at which $x/D = 9$ and then becomes slower compared to the undisturbed fully developed flow. An inflection point appears in the inner region of the mean velocity profile in the k-type flow over the initial recovery stage, i.e., $x/D = 0.1$ to 4. This inflection point propagates steadily toward the center of the pipe. Otherwise, the mean velocity profile after the d-type roughness is occurring in shape with no inflection point. The velocity profiles containing inflection points indicate that a large mixing effect occurred as a result of the presence of k-type roughness. One difference in the roughness effect between d- and k-type roughness is expected to be that flow over k-type roughness produces vortices shedding from the grooves, whereas this does not happen for the d-type roughness.

3.2 Characteristic thicknesses

Setting the definition of axisymmetric cylindrical flow for displacement thickness, δ_d and momentum thickness, δ_m and energy thickness, δ_e as follows:

$$\delta_d = \int_0^R \left(1 - \frac{U}{U_c}\right)\left(\frac{r}{R}\right) dr. \tag{3.2}$$

$$\delta_m = \int_0^R \frac{U}{U_C}\left(1 - \frac{U}{U_c}\right)\left(\frac{r}{R}\right) dr. \tag{3.3}$$

$$\delta_e = \int_0^R \frac{U}{U_C}\left(1 - \frac{U^2}{U_c^2}\right)\left(\frac{r}{R}\right) dr. \tag{3.4}$$

The momentum integral equation of axisymmetric cylindrical flow can be expressed as follows:

$$\frac{d\delta_m}{dx} = \frac{C_f}{2} - (2 + H)\frac{\delta_d}{U_c}\frac{dU_c}{dx}\ , \tag{3.5}$$

where shape factor, H is the ratio of displacement thickness to momentum thickness. This momentum integral Equation (3.5) is identical in form with the same relation for an incompressible, two dimensional boundary layer flow subject to a pressure gradient (see Ward -Simth[11] and Schlichting[12]).

The momentum boundary layer thicknesses, as obtained using Equation (3.3), for two types of roughness are shown in Fig. 7. For the shortest roughness length of the d-type flow, the momentum thickness is apparently the same as the undisturbed fully developed flow. For longer roughness lengths, the variation in the

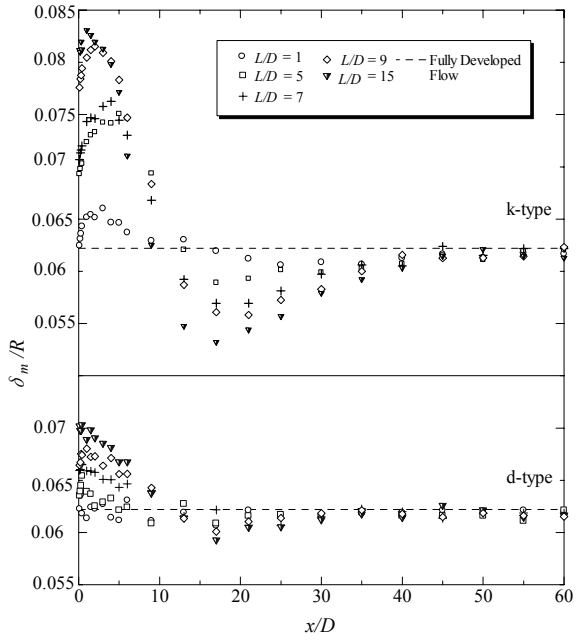

Fig. 7 Momentum thickness of two types of roughness appearing in the downstream of the flow

momentum thickness shows an overhang and then recovers downstream. The overhang appears more clearly for the k-type flow as compared to the d-type. For both flow types, undershoot of the thickness can be observed over the region of $x/D = 17\sim21$.

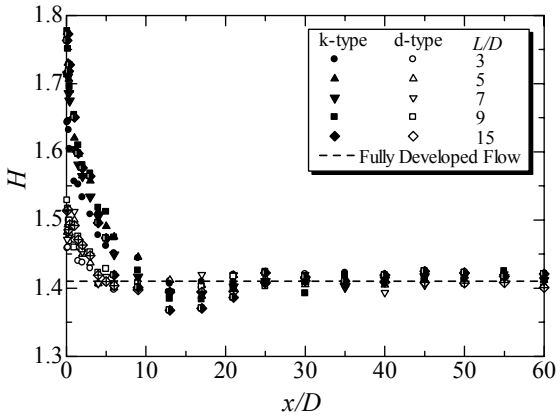

Fig. 8 Comparison of shape factor of two types of roughness varying in length

The momentum integral of Equation (3.5) states that the variation in momentum thickness is affected by the wall friction force and the pressure gradient. In the initial stage of the recovery process, the inflection point in the mean velocity profile may be an indication of the overhang behavior in the momentum thickness variation for the k-type roughness. The high shear layer usually is accompanied with large Reynolds shear stress which keeps higher momentum transport and turbulent production after the end of the rough wall disturbance.

Comparison of shape factor, H of two types of rough wall is shown in Fig. 8. The experimental data shows the quite different profile of two rough wall flows. It could be explained that the effect of wall friction, i.e., larger wall friction of k-type roughness tends to cause larger velocity defect and larger effective pressure drop as compare to d-type., Range of 1.65 to 1.78 for k-type and of 1.46 to 1.53 for d-type of maximum value of shape factors are found after the rough wall. Shape factor of k-type rough wall flow falls dramatically than d-type because of the high momentum transport was occurred by the effect of roughness, i.e. the overhung structure of momentum thickness in Fig. 7. Even though displacement thickness and momentum thickness depend on the roughness length, the boundary layer ratio, shape factor is found to be weak dependence. This could happen on the different wall roughness conditions which turn to cause different local shear effects on each flow.

Fig. 9 compares three types of boundary layer thickness under the same effective pressure drop obtained using Equations (3.2) through (3.4). For all thicknesses, similar behaviors, including rapid decrease, undershoot, and approaching the equilibrium value, are observed downstream of the roughness section. The surface condition of the pipe is smooth-to-rough-to-smooth (S-R-S), the mean flow decelerates near the wall and accelerates in the core region. The momentum is reduced near the wall by the large wall shear stress over the roughness section. The mean velocity in the core region is accelerated due to the fluid displacement from the

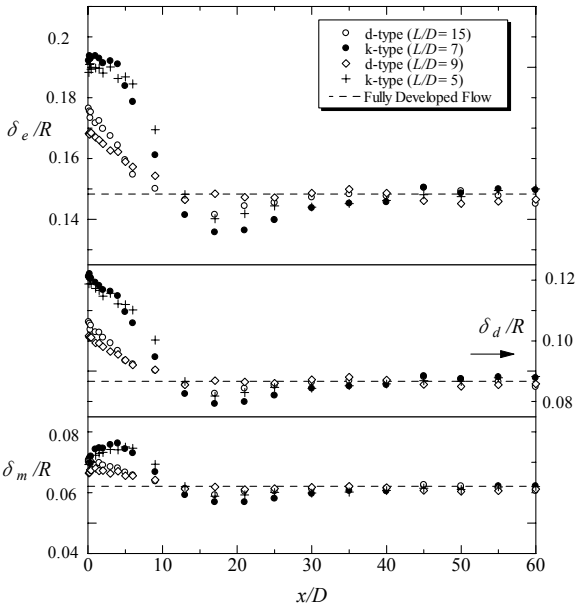

Fig. 9 Comparison of three types of boundary layer thickness under same effective pressure drop

near wall region. In the recovery process, the Reynolds shear stress enhanced by the roughness strongly transported streamwise momentum toward the wall. The enhanced Reynolds shear stress increased the turbulence by converting the kinematic energy from the mean flow to turbulence.

The undershoot phenomenon occurs at $x/D = 17\sim21$ for all boundary layer thicknesses. The experimental results show that the streamwise distance from the starting point of recovery to undershoot is independent of the strength and type of roughness. In Fig. 6, the core velocities are slower than in the fully developed flow. Since the flow rate is constant, the velocities near the wall should be faster than in undisturbed fully developed flow. Except in the initial stage, the pace of the recovery process is determined by the large-scale motion, where the length scale is comparable to the pipe diameter.

In Fig. 9, although start with the almost same value at the first measurement point, stronger influence of the wall friction for the k-type roughness leads to appear impulse shape in the momentum thickness. As shown in Fig. 6, the inflection point in the mean velocity profile propagates toward the center of the flow. This suggests that larger mixing occurred as a result of the flow response to the k-type roughness. Consequently, the stress bore phenomenon may occur for the Reynolds shear stress of the k-type roughness flow, and these stress bores will interact with the velocity gradients of the mean flow. The stress bore phenomenon is a result of turbulent transport and interaction between the turbulence and the mean flow (Andreopoulos and Wood[3]). This could be proved in the energy thickness of k-type roughness, because the turbulent production is involved in integral of the mean kinematic equation and contribute to increase of energy thickness. Even though the effective pressure drop is the same, the energy thickness of the k-type roughness is larger than that of the d-type roughness.

For both types of roughness peak values of the momentum thickness, $(\delta_m)_P$, and minimum values of the momentum thickness, $(\delta_m)_N$, were plotted as functions of the effective pressure drop in Fig. 10. Peak values for the d-type roughness flow appear to be proportional to the pressure drop. The enhancement of the peak values of the k-type roughness flow appears to reach the saturated condition at the two longest lengths $(L/D = 12\ and\ 15)$. The minimum values of momentum thickness for both types of roughness are approximately constant until 0.15 of ΔC_P. For both types of roughness flow in which ΔC_P is less than 0.15, the minimum values of the momentum thickness are found not to exceed $\pm2.5\%$ of the undisturbed fully developed flow, i.e., undershoot does not occur.

The recovery length, x_r is difficult to define because the flow parameters tend to approach their equilibrium values after several oscillations about these final values (Logan et al.[1]). They could not determine the recovery length because the length of the test section was insufficient. In the present study, after the roughness section, the mean flow recovered to the fully developed flow condition. The recovery condition was set to $\pm2.5\%$ of the undisturbed fully developed value, i.e., the recovery condition was on the same order of uncertainty as the corresponding thickness. The

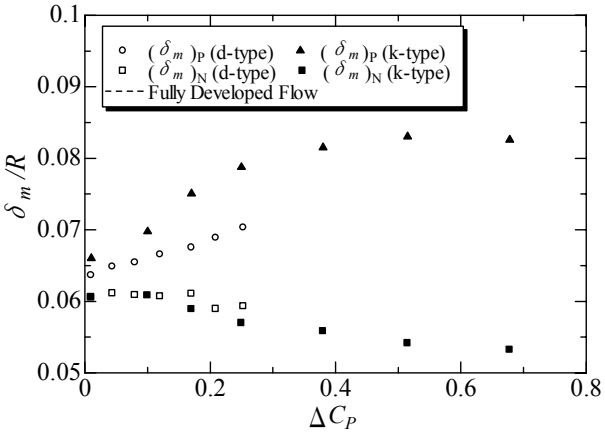

Fig. 10 Peak and minimum values of momentum thickness against effective pressure drop

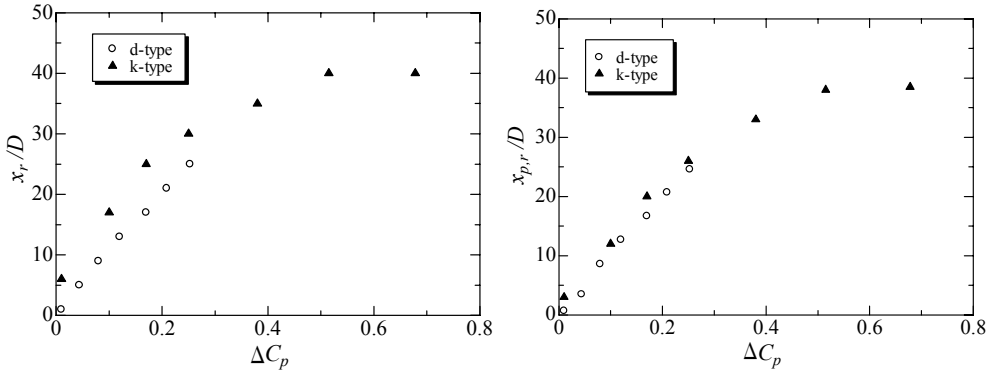

(a) (b)

Fig. 11 (a) Recovery length of the system depend on effective pressure drop; (b) Length between peak and recovery condition varying in effective pressure drop

recovery length for both types of roughness plotted in terms of the effective pressure drop is shown in Fig. 11(a). In this figure, the recovery lengths of both types of roughness appear to follow different trends. At $L/D = 12$, the total recovery length of the k-type roughness likely reaches the saturated condition $40D$ after the roughness section. As shown in Fig. 12(b), the internal boundary layer merges approximately at the pipe centerline.

The distance measured from the peak value of each boundary layer to the recovery condition was defined as $x_{p,r}$, which is plotted as a function of the effective pressure drop in Fig. 11(b). The trends for both types almost collapse. The single curve proves that different responses due to roughness appear only in the initial stages and that the total recovery length can be determined uniquely by the effective pressure drop.

After the roughness, the relaxation process takes place downstream of the flow. The geometry of the roughness (cavity) is different, e.g., the wall shear stress and pressure drag are different. Therefore, the initial stages of the boundary layer thickness are quite different. The wall shear stress of the k-type roughness is expected to be noticeably large. The movement of fluid particles in the pipe was caused by the pressure drop. On the other hand, the total recovery length uniquely depends on the effective pressure drag. The effective pressure drop can be considered as extra energy input into the mean kinematic energy. The extra energy will be converted to turbulent kinematic energy and transported to smaller scale eddies at the end of the energy cascade. The properties of roughness will vanish in the cascade process. The time from input to dissipation is related to the spectral bandwidth of the undisturbed fully developed flow.

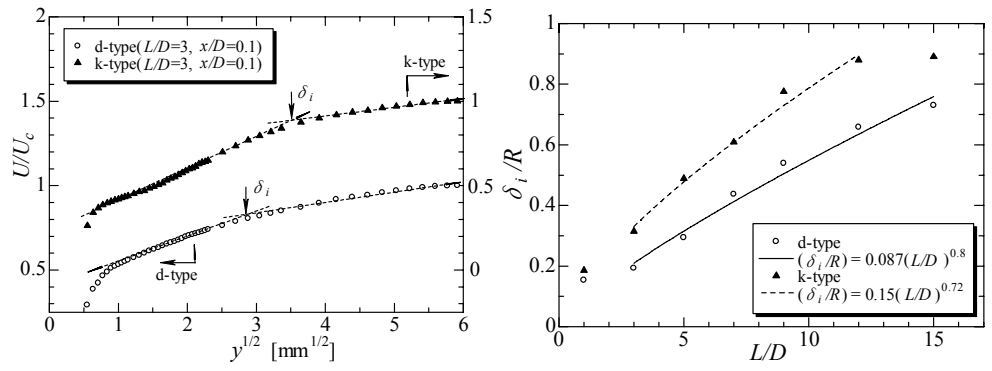

(a) (b)

Fig. 12 Development of the internal boundary layer; (a) Mean velocity profile plotted as a function of $y^{1/2}$; (b) Development of internal boundary layer plotted as a function of roughness length

3.3 Internal boundary layer development

The edge of the internal boundary layer was approximated using the knee point detection method, and the intersection of the straight lines in the half-power plot is shown in Fig. 12(a). The mean velocity profile inside the internal layer in the region near the step exhibits a linear trend when plotted in the form $U\ vs.\ y^{1/2}$. The intersection of two straight lines is found to be closely related to the edge of the internal boundary layer (Antonia and Luxton[13]). After one step, the new wall condition generates a new internal boundary layer that grows out of the original layer. The height of the new internal boundary layer, δ_i, is the distance above the wall at which the mean velocity profile merged with the corresponding profile of a reference layer that developed under the same conditions, but without the change in wall roughness. In a number of studies, measurement in such a reference layer was not performed, although such measurement in a reference layer was often unnecessary (Schofield[14]).

The value of the first measurement point, $x/D = 0.1$, for all roughness lengths plotted against the dimensionless roughness length are shown in Fig. 12(b). The new internal boundary layer propagates toward the center of the pipe downstream of the roughness section. The flow over the k-type roughness section propagates much faster than that over the d-type roughness section. Fitting the results yielded $(\delta_i/R)\sim(L/D)^{0.72}$ for the k-type roughness and $(\delta_i/R)\sim(L/D)^{0.82}$ for the d-type roughness.

In internal flows, the effect of wall roughness appears in the core region or the outer layer because the flow rate must be constant by virtue of the continuity condition. After k-type roughness, the thickness of the internal boundary layer almost reaches the center of the pipe at $L/D \geq 12$, where the total recovery length is independent of the effective pressure drop and the length of the roughness. Development of the internal boundary layer is important for describing and classifying the effect of the length of the roughness.

4. Conclusions

At the same effective pressure drop, high-mixing effects of the flow over k-type roughness is noticeably larger, which can be seen as an inflection in the mean velocity profile. A clearer impulse structure appears in the initial recovery stage of momentum thickness of the flow after the k-type roughness section, which indicates that stress bore phenomena will occur in the Reynolds shear stress profile. Even for the same effective pressure drop, the turbulent energy production is lower for the d-type roughness than for the k-type roughness.

The total recovery length from the roughness disturbance depends only on the magnitude of the effective pressure drop, ΔC_p. The maximum total recovery length was found to be $40D$ downstream of the roughness at $L/D \geq 12$, where the internal boundary layer merges approximately at the pipe centerline.

References

(1) Logan, E. and Phataraphruk, P., Mean flow downstream of two dimensional roughness elements, Trans. ASME, J. Fluid Mech., Vol. 111, (1989), pp.149-153.
(2) Smits, A.J. and Wood, D.H., The Response of Turbulent Boundary Layers to Sudden Perturbations, Annu. Rev. Fluid Mech., Vol. 17, (1985), pp.321-358.
(3) Andreopoulos, J and Wood, D.H., The response of a turbulent boundary layer to a short length of surface roughness, J. Fluid Mech., Vol. 118, (1982) pp. 143-164.
(4) Leonardi. S., Orlandi. P., Antonia, R.A, Properties of d- and k-type roughness in a turbulent channel flow, Physics of Fluids, Vol. 19, (2007), 125101.

(5) Perry, A.E., Schofield, W.H. and Joubert, P.N., Rough wall turbulent boundary layer, J. Fluid Mech., Vol. 37, (1969), pp. 383-413.
(6) Kameda, T., Osaka, H. and Mochizuki, S., Turbulent structure in the vicinity of roughness element for boundary layer over a k-type rough wall, Transaction of JSME, Series B, Vol. 66, No. 646, (2000), pp. 1347-1355.
(7) Tani, I., Turbulent boundary layer development over rough surfaces, Perspectives in Turbulence Studies, Springer-Verlag, (1987), pp. 223-249.
(8) Chue, S. H., Pressure probes for fluid measurement, Prog. Aerospace Sci., Pergamon Press, Vol. 16, No. 2, (1975), pp. 147-223.
(9) Benedict, R.P., Fundamental of pipe flows, A willy interscience publication, (1980), pp.133-175, 233-242.
(10) Nagib, H.M and Chauhan K.A., Variations of von Kármán coefficient in canonical flows, Physics of Fluid, Vol. 20, (2008), 101518.
(11) Ward-smith, A. J., Internal fluid flow (The fluid dynamics of flow in pipes and ducts), Oxford University Press, (1980), pp. 229-247.
(12) Schlichting, H., Boundary-layer theory, McGraw-Hill, 7th ed., (1979), pp. 158-162.
(13) Antonia, R.A. and Luxton, R.E., The response of a turbulent boundary layer to a step change in surface roughness: Part 1. Smooth to rough, J Fluid Mech., Vol. 48, No. 4, (1971), pp. 721-761.
(14) Schofield, W.H., The Response of turbulent shear flow to discontinuous changes in surface roughness, Mech. Eng. Report 150, Aeronautical Research Lab, Melbourne, Australia, (1977).